

# Lithium niobate–tantalate thin films on Si by thermal plasma spray CVD

S.A. Kulinich<sup>a,\*</sup>, H. Yamamoto<sup>b</sup>, J. Shibata<sup>c</sup>, K. Terashima<sup>a,b</sup>, T. Yoshida<sup>a</sup>

<sup>a</sup>Department of Materials Engineering, Faculty of Engineering, The University of Tokyo, 7-3-1 Hongo, Bunkyo-ku, 113-8656 Tokyo, Japan

<sup>b</sup>Department of Advanced Materials Science, Graduate School of Frontier Science, The University of Tokyo, 7-3-1 Hongo, Bunkyo-ku, 113-8656 Tokyo, Japan

<sup>c</sup>Engineering Research Institute, The University of Tokyo, 2-11-16 Yayoi, Bunkyo-ku, 113-8656 Tokyo, Japan

## Abstract

Highly (0 0 6)-oriented lithium niobate–tantalate ( $\text{LiNb}_{0.5}\text{Ta}_{0.5}\text{O}_3$  and  $\text{LiNb}_{0.2}\text{Ta}_{0.8}\text{O}_3$ ) thin films with submicron thickness were prepared by thermal plasma spray CVD on Si(1 0 0) substrates covered with a native oxide layer. The effect of the growth rate on film orientation and surface morphology has been studied. It was shown that both growth temperature and growth rate are responsible for producing highly (0 0 6)-textured films. The films do not exhibit any effect of the Nb/Ta ratio on their orientation. © 2002 Elsevier Science B.V. All rights reserved.

PACS: 81.15.Gh; 68.55.-a

Keywords: Growth rate; Thermal plasma spray CVD; Thin films;  $\text{LiNb}_{1-x}\text{Ta}_x\text{O}_3$

## 1. Introduction

To date, applications of the unique physical properties of lithium niobate ( $\text{LiNbO}_3$ , LN) and lithium tantalate ( $\text{LiTaO}_3$ , LT), including large second-order optical non-linearity, piezoelectric, pyroelectric and elasto-optic effects, have been limited to devices fabricated from bulk crystals. Recently, ferroelectric oxide thin films have attracted great interest for various applications, including nonvolatile memory, infrared sensors, optical high-speed switches and ultrasonic transducers. Their many advantages are due to their suitability for weak electric fields and to their potential for use in complex structures on the nanometric scale [1–5].

Lithium niobate–tantalate ( $\text{LiNb}_{1-x}\text{Ta}_x\text{O}_3$ , LNT) is the solid solution of LN and LT and therefore possesses intermediate properties, which vary with the  $x = \text{Ta}/(\text{Nb} + \text{Ta})$  ratio, from those of LN ( $x = 0$ ) to those of LT ( $x = 1$ ). This makes it, in some cases, an even more attractive material than the pure compounds, since its physical properties are governed, to a large extent, by the Nb/Ta ratio and thus can be tuned to meet engi-

neering specifications, which is very important for practical applications [6,7].

From the technological viewpoint,  $\text{LiNb}_{1-x}\text{Ta}_x\text{O}_3$  ( $x = 0–1$ ) films on silicon or other semiconductors are very promising, because they would permit an integration of wave-guiding electrooptic circuits with their attendant semiconductor electronics [4,8]. To exploit the optical properties of these materials and the superior electrical properties of silicon, it is of great importance to fabricate highly (0 0 6)-textured LNT films on Si substrates, for both metal-ferroelectric-semiconductor nonvolatile memory and optoelectronic applications [8,9]. In the past decade, numerous attempts at depositing thin films of LN and LT on Si substrates by various techniques have been reported [4,8,10–15]. However, there is little information on the crystallinity of these films [4], and there are only a few reports on LNT films on Si substrates [9,16].

Thermal plasma spray CVD (TPS CVD) was first applied for deposition of ferroelectric thin films by Yamaguchi et al. [17], who demonstrated the effectiveness of the method for high-rate deposition of LN films on (1 1 0) sapphire and large-area deposition on 5-inch Si(1 1 1) substrates. Since the substrate temperature could not be controlled in their large-area experiment, different LN film qualities and orientations were

\*Corresponding author. Tel./fax: +81-3-5841-7103.

E-mail address: kulinich@terra.mm.t.u-tokyo.ac.jp (S.A. Kulinich).

Table 1  
Summary of experimental conditions

Source Li:Nb:Ta ratio	2:1:1; 5:1:4
Power, kW	46.2
Pressure, Torr	150
O <sub>2</sub> tangential gas flow rate, l/min	45.0
Ar carrier gas flow rate, l/min	3.0
Ar spray gas flow rate, l/min	3.6
Ar inner gas flow rate, l/min	5.0
Liquid feeding rate ( <i>R</i> ), ml/min	0.5–8.0
Deposition temperature, °C	520–600
Torch-substrate distance ( <i>L</i> ), cm	37
Deposition time, min	0.5–8.0
Substrate	Si(1 0 0)
LNT film thickness, nm	160–180

observed for various Si wafer areas. Recently, the TPS CVD technique has been applied by our group to epitaxial LiNb<sub>1-x</sub>Ta<sub>x</sub>O<sub>3</sub> ( $x=0-0.7$ ) films on (0 0 1) sapphire [18–20] and to (0 0 6)-oriented LiNb<sub>0.5</sub>Ta<sub>0.5</sub>O<sub>3</sub> films on Si(1 1 1) and Si(1 0 0) [16]. In our previous work, we carefully studied the role of the deposition temperature ( $T_{\text{sub}}$ ) in producing highly (0 0 6)-oriented LiNb<sub>0.5</sub>Ta<sub>0.5</sub>O<sub>3</sub> films on Si substrates [16]. In this work, we investigate the influence of the liquid source feeding rate (and consequently, growth rate) on film orientation and surface roughness. We also demonstrate the growth of LNT films with  $x>0.5$  and good (0 0 6)-texture, which is the first successful attempt on Si wafers reported so far.

## 2. Materials and methods

LiNb<sub>1-x</sub>Ta<sub>x</sub>O<sub>3</sub> films with  $x=0.5$  and  $x=0.8$  were prepared by the TPS CVD technique. The setup with upward-blowing O<sub>2</sub>–Ar radio-frequency inductively-coupled plasma has been described earlier [18,19]. The main details of the deposition procedure, as well as the main characteristics of the method, have also been presented elsewhere [17–19]. A summary of the main experimental conditions is given in Table 1. The as-used substrates were 10×10×0.5 mm<sup>3</sup> Si(1 0 0) wafers with a native SiO<sub>2</sub> layer. Prior to film fabrication, they were ultrasonically cleaned and rinsed with acetone and ethanol solvents. As previously reported by us [16], the LiNb<sub>0.5</sub>Ta<sub>0.5</sub>O<sub>3</sub> films demonstrate no effects of the nature of the Si(1 1 1) or Si(1 0 0) substrate or of the SiO<sub>2</sub> cladding layer thickness on their orientation and crystallinity. This is why only one type of Si wafer was used in the present work.

Accurately measured volumes of the reagent-grade lithium–niobium and lithium–tantalum double-alkoxide metalorganic solutions (LiNb(OR)<sub>6</sub> and LiTa(OR)<sub>6</sub> in 3-methylbutyl acetate solvent from Kojundo Chemical Lab. Co., Japan, commercially available for dip coating) were mixed in appropriate ratios and then used as the liquid source material. The concentrations of metals (Li

and Nb or Li and Ta) in individual precursor solutions, which were then mixed in appropriate ratios, corresponded to 3 wt.% LiNbO<sub>3</sub> or 3 wt.% LiTaO<sub>3</sub>, respectively. In earlier papers, we reported that the composition of deposited LNT films (Nb/Ta ratio) was very close to that of sprayed liquid precursors [16,18–20], therefore in this study two mixtures with the Nb:Ta ratios of 1:1 and 1:4 were used to produce the films with the compositions LiNb<sub>0.5</sub>Ta<sub>0.5</sub>O<sub>3</sub> and LiNb<sub>0.2</sub>Ta<sub>0.8</sub>O<sub>3</sub>, respectively.

In order to examine the LNT film orientation, crystallinity and phase composition, X-ray diffraction (XRD) was used. Film thickness was examined by cross-sectional scanning electron microscopy (SEM) and transmission electron microscopy (TEM). Surface morphology was analyzed by SEM and atomic force microscopy (AFM). The microstructure and interface between the film and the substrate were studied using TEM; energy-dispersive X-ray spectroscopy (EDS) with a 2 nm probe was applied to chemical analysis.

## 3. Results and discussion

In accordance with the approach of Hu et al. [15], a convenient parameter for describing the degree of (0 0 6) orientation of the LNT films (orientation factor or *c*-axis orientation degree) on Si substrates can be defined by

$$f = \frac{I_r(0\ 0\ 6) - I_r^{\text{powder}}(0\ 0\ 6)}{1 - I_r^{\text{powder}}(0\ 0\ 6)}$$

where the relative intensity  $I_r(0\ 0\ 6)$  is the intensity of the (0 0 6) peak normalized by the total intensity of all the peaks of LNT between  $2\theta=20^\circ$  and  $60^\circ$ . For randomly oriented polycrystalline films, as in the case of powders, the degree of *c*-axis orientation (*f*) is equal to 0; for completely (0 0 6)-oriented LNT films,  $f=1$  and for partially (0 0 6)-textured films, *f* falls between 0 and 1 [9,13,15,19]. Hereinafter, this parameter is also used in this work.

Since the orientation of LiNb<sub>0.5</sub>Ta<sub>0.5</sub>O<sub>3</sub> films on both Si(1 1 1) and Si(1 0 0) substrates has been shown in our previous work [16] to be strongly governed by the deposition temperature  $T_{\text{sub}}$ , and (0 1 2)-textured films are generally grown at  $T_{\text{sub}}>600^\circ\text{C}$ , in this study we used only  $T_{\text{sub}} < 600^\circ\text{C}$ .

Fig. 1a shows the XRD pattern for the LiNb<sub>0.2</sub>Ta<sub>0.8</sub>O<sub>3</sub> film deposited at  $R=2$  ml/min and a relatively low temperature of  $T_{\text{sub}}=520-540^\circ\text{C}$  and then in situ annealed at  $565^\circ\text{C}$  for 5 min. Besides a strong (0 0 6) LNT peak, two peaks which belong to the Li-rich Li<sub>3</sub>(Nb,Ta)O<sub>4</sub> (LR,  $2\theta=37^\circ$ ) phase and the Li-deficient Li(Nb,Ta)<sub>3</sub>O<sub>8</sub> (LD,  $2\theta=44.4^\circ$ ) phase are visible. For comparison, the XRD pattern of the LiNb<sub>0.5</sub>Ta<sub>0.5</sub>O<sub>3</sub> film fabricated at  $R=4$  ml/min and optimal  $T_{\text{sub}}=565-580^\circ\text{C}$  is also given in Fig. 1b; the

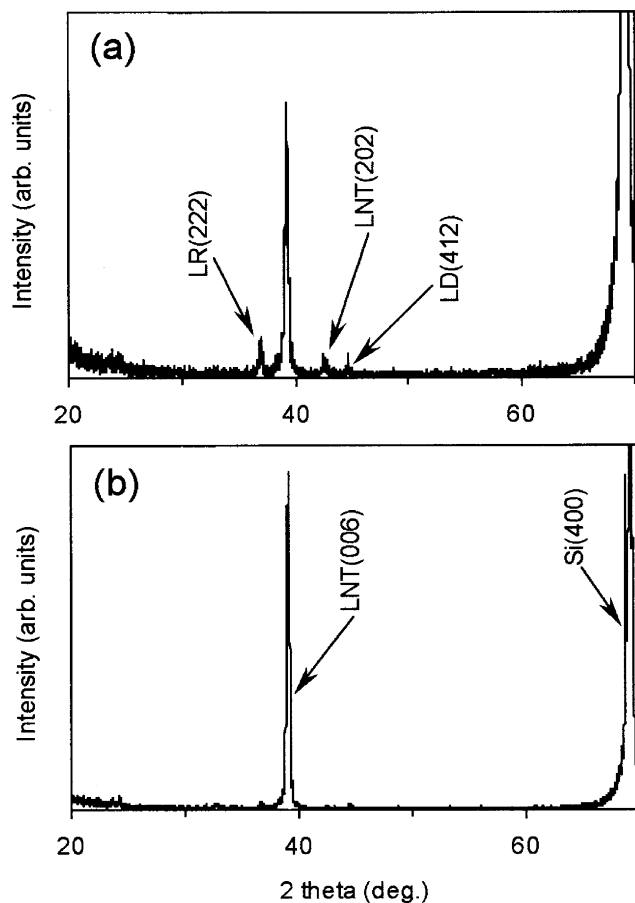


Fig. 1. XRD patterns of highly (006)-oriented  $\text{LiNb}_{0.2}\text{Ta}_{0.8}\text{O}_3$  (a) and  $\text{LiNb}_{0.5}\text{Ta}_{0.5}\text{O}_3$  (b) films deposited onto  $\text{Si}(1\ 0\ 0)$  substrates. Film (a) was fabricated at  $R=2$  ml/min for 2 min and at  $T_{\text{sub}}=520\text{--}540$  °C; and film (b) was formed at  $R=4$  ml/min for 1 min at  $T_{\text{sub}}=565\text{--}580$  °C. Both were annealed at 565 and 590 °C for 5 min, respectively.

film had  $f=0.97$ . It is seen that the LNT films deposited at low substrate temperatures have slightly non-uniform chemical and phase compositions, and therefore higher  $T_{\text{sub}}$  or subsequent in situ annealing is necessary. On the other hand, the upper optimal deposition temperature is limited by the change to the (012)-texture (e.g. optimal  $T_{\text{sub}} < 590$  °C at  $R=4$  ml/min [16]). Such chemical and phase inhomogeneities are believed to result from the fast deposition and relatively low surface and volume species mobility in the temperature range from 520 to 540 °C. At higher deposition temperatures, the atomic diffusion becomes faster, which results in a decrease of the LR and LD peak intensities and better film compositional homogeneity. For the same reason, in situ  $\text{O}_2\text{--Ar}$  plasma annealing was used to increase film crystallinity and phase homogeneity. It is noteworthy that the formation of either the LR or LD phase during LN or LT deposition onto a Si or sapphire substrate has been reported by many groups [11,21], however, this appears to be the first report thus far on their simultaneous formation.

The growth rate employed in vapor phase deposition techniques seems to be very important with regard to LNT film (006) orientation, the films' quality and surface smoothness on Si substrates. For example, when the growth rate applied by Lee and Feigelson [4] in the metalorganic CVD (MOCVD) method was increased from 2 nm/min to 4–5 nm/min, considerable improvement in the (006) texture of LN films on  $\text{SiO}_2/\text{Si}$  wafers could be achieved, while the relative fraction of the (012)-textured grains decreased. It was also shown that the LN film surface smoothness could be controlled by varying the film growth rate on both Si and sapphire wafers [4,5]. Again, the growth rate of 0.5 nm/min for RF magnetron-sputtered LN films in Huang and Rabson's work [10] gave only (104) orientation, while Rost et al. [21], who also used RF magnetron sputtering, achieved high (006) orientation at 1.5 nm/min. As discussed below, since no particular lattice relationship is expected between LNT film and Si or amorphous  $\text{SiO}_2$  in the (006)-oriented LNT film, it should be concluded that such an orientation results principally from the growth kinetics of the highly anisotropic LNT material in any vapor phase deposition method. This is in good agreement with the numerous difficulties of sol-gel techniques, where growth rate anisotropy (see below) cannot be used, related to the fabrication of highly (006)-textured LNT films on silicon [9,22,23].

The change in LNT film  $c$ -axis orientation degree as a function of liquid source feeding rate  $R$  (and consequently growth rate) is shown in Fig. 2a; in the experiments presented here, only the  $R$  parameter and deposition time were varied at  $T_{\text{sub}}=560\text{--}575$  °C. The phase composition and crystallite orientation of the LNT films were analyzed by XRD using a  $\theta\text{--}2\theta$  scanning mode;  $\theta$  scanning was used to estimate film crystallinity (rocking-curve measurement). Since these XRD results are affected by film thickness, all samples in the series were grown to have similar thicknesses in the range of 160–180 nm. The LNT films were deposited for an appropriate period of time (from 0.5 to 8 min) and then were in situ annealed in  $\text{O}_2\text{--Ar}$  plasma at the deposition temperature for 5 min. As shown in Fig. 2a, LNT film texturing (orientation factor  $f$ ) was found to increase with increasing feeding rate up to approximately 4 ml/min, indicating better (006) crystalline alignment, probably caused by the suppression of adspecies surface mobility and the growth rate anisotropy, as described below. This result was expected, because  $T_{\text{sub}}=560\text{--}575$  °C was shown to be the optimal deposition temperature for obtaining highly (006)-oriented LNT films at  $R=4$  ml/min [16]. When the feeding rate exceeded  $R=4$  ml/min, some deviation of the (006) orientation degree was observed, indicating some worsening of the (006) texture. Such a behavior can be attributed to the

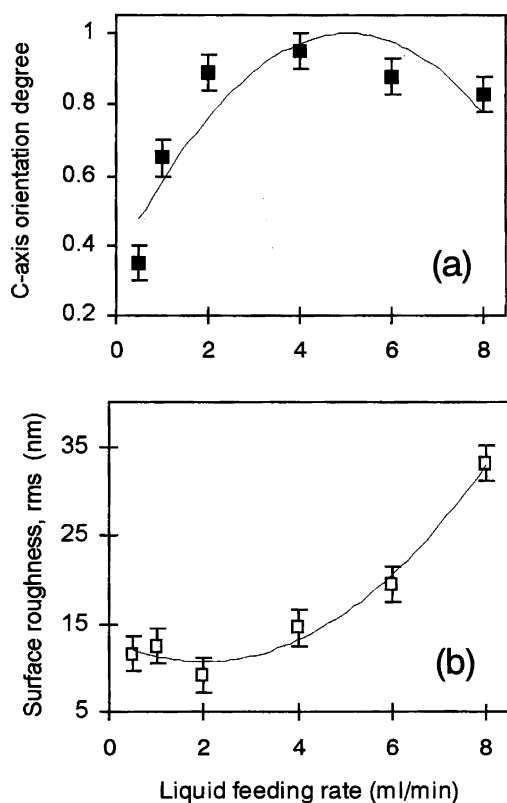


Fig. 2. Change of *c*-axis orientation degree (a) and surface r.m.s. roughness (b) as functions of liquid feeding rate *R* employed for  $\text{LiNb}_{0.5}\text{Ta}_{0.5}\text{O}_3$  films. The deposition temperature  $T_{\text{sub}}$  was 560–575 °C. Solid lines are added only as guides for the eye.

contribution of a number of factors, e.g., less reliable temperature control at higher feeding rates (for comparison:  $\pm 10$  °C at  $R=8$  ml/min, whereas it was  $\pm 5$  °C at  $R=4$  ml/min) or gas phase nucleation formation of larger clusters/particles at higher source material concentrations in plasma.

Generally, in the case of film growth on an amorphous substrate (without epitaxy), texture may evolve as the result of the preferential growth of some grains with a certain crystallographic orientation. To describe such a dominant growth of some crystallites, two main models have been developed, according to the surface diffusion conditions. The first model proposes that the nuclei are all initially randomly oriented on the substrate and that, as they subsequently expand uniformly in time, the grains with their fastest growth direction oriented most closely to the substrate normal consume those with lower projected growth rates. This mechanism, also called ‘competitive growth’ or ‘survival of the fastest’, is based on growth rate anisotropy and occurs at relatively low temperatures where the diffusivity is low at the outer surface of the growing film [4,24]. The other model is more appropriate for relatively high temperatures and is based on the tendency for the surface to lower its surface energy (surface free energy anisotropy), as one of the physical laws governing the evolution of texture, when the surface mobility of the species is sufficiently high [4,25].

As suggested by Wu et al. [14], the (0 1 2) plane is the lowest LNT energy plane. Therefore, at higher deposition temperatures, nuclei on the surface tend to rearrange themselves so as to minimize the total surface energy and to form the (0 1 2)-textured grains, which was in fact observed for TPS-CVD-grown LNT films on  $\text{SiO}_2/\text{Si}$  at  $T_{\text{sub}} > 600$  °C [16]. The high (0 0 6) orientation of the LNT films in Figs. 1 and 2, from the above point of view, can be ascribed to the fastest growth rate of the (0 0 6)-plane, which is well consistent with reference [4]. Furthermore, the increased feeding rate at the same  $T_{\text{sub}}$  is expected to suppress surface mobility, thus improving the (0 0 6) orientation, and this is evident in Fig. 2a at  $0.5 < R < 4$  ml/min. Again, it can be expected that the (0 0 6) texture for LNT films deposited at a low feeding rate of  $R=0.5$  ml/min will be improved by adopting  $T_{\text{sub}} < 560$  °C; this was indeed confirmed by depositing LNT film with  $f=0.92$  at  $T_{\text{sub}}=545\text{--}555$  °C, the cross-section of which is shown in Fig. 3.

It is noteworthy that a highly similar tendency was reported by Lee and Feigelson for LN/Si film texturing dependent on growth rate at a constant deposition temperature [4]. In their MOCVD experiment, when faster growth rates (4–5 nm/min) were used, (0 0 6) orientation could be improved, and the formation of (0 1 2) grains was significantly retarded compared to the case of using slower growth rates (1.5–2 nm/min). Since the LNT film crystallinity is governed in many respects by the degree of orientation, the narrowest (0 0 6) rocking-curve full-width at half-maximum

is reported by Lee and Feigelson for LN/Si film texturing dependent on growth rate at a constant deposition temperature [4]. In their MOCVD experiment, when faster growth rates (4–5 nm/min) were used, (0 0 6) orientation could be improved, and the formation of (0 1 2) grains was significantly retarded compared to the case of using slower growth rates (1.5–2 nm/min).

Since the LNT film crystallinity is governed in many respects by the degree of orientation, the narrowest (0 0 6) rocking-curve full-width at half-maximum

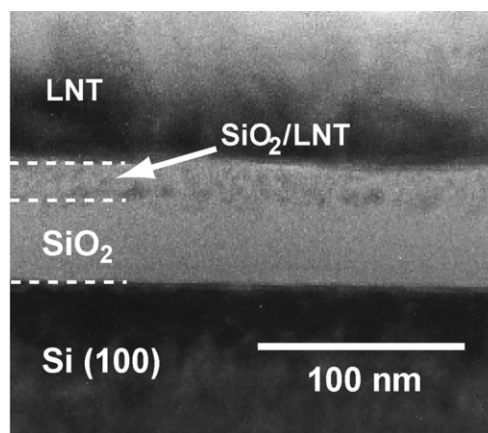


Fig. 3. A cross-sectional TEM image revealing the interface between the 180-nm-thick  $\text{LiNb}_{0.5}\text{Ta}_{0.5}\text{O}_3$  film (deposited at  $R=0.5$  ml/min and  $T_{\text{sub}}=545\text{--}555$  °C for 8 min) and  $\text{SiO}_2/\text{Si}$  substrate; the film is highly (0 0 6)-oriented:  $f=0.92$ . Interface area including Si wafer, amorphous  $\text{SiO}_2$ , amorphous intermediate layer  $\text{SiO}_2/\text{LNT}$  and crystalline LNT film (separated by dashed lines) is shown.

(FWHM) achieved for the series in Fig. 2 was obtained in the film with the highest (0 0 6) texture (deposited at  $R=4$  ml/min) and was equal to  $3.5^\circ$ , which is very close to our previously reported value [16]. Thus far, the lowest (0 0 6) rocking-curve FWHM value reported for the LN films fabricated on Si substrates is  $1.8^\circ$  [4]. Even though our best value for LNT film is relatively large, we consider it to be rather good, particularly when taking into account the very high growth rate of the films and the fact that in situ annealing temperature and time may be further optimized which can further improve film crystallinity. Note that the growth rates applied in this study were approximately 20–350 nm/min for  $R=0.5$ –8 ml/min, respectively, which is 10–100 times faster than those for most conventional vapor phase deposition techniques.

Fig. 2b shows the variation of the LNT film surface root mean square (r.m.s.) roughness with the deposition liquid feeding rate  $R$  for the same series as in Fig. 2a. Although visually all the films are mirror-like, when the liquid source input was increased to  $R < 4$  ml/min, an increase of their surface r.m.s. roughness was observed; only at lower  $R$  it was approximately 10–15 nm. The reason for such behavior of the LNT film surface vs. growth rate is still unclear and additional investigation is required. One possible explanation for this increase of roughness, by analogy with MOCVD results [4], is vapor phase nucleation and subsequent embedment of larger LNT particles into the growing film at higher material concentrations in plasma, as mentioned above. Another possible explanation of the surface roughening is the amorphous interlayer between the film and substrate, whose thickness and structure may influence subsequent crystalline LNT film formation, growth and surface morphology (see below). The results in Fig. 2b clearly indicate that controlling the growth rate (or source feeding rate) may be a key factor in varying the LNT film surface morphology. Surface images of mirror-like LNT films on  $\text{SiO}_2/\text{Si}$  substrates observed by SEM and AFM revealed that their surface did not contain any cracks or other serious defects. However, as seen in Fig. 2b and as mentioned in our previous work [16], the roughness of the high-growth-rate TPS-CVD-prepared LNT films is still higher than that of the best LN and LT samples reported so far [4,5], which implies that further investigations on nucleation and growth processes are required in order to improve the LNT film surface smoothness.

Fig. 3 shows a cross-sectional TEM image and reveals the interface structure of  $\text{LiNb}_{0.5}\text{Ta}_{0.5}\text{O}_3$  film deposited at  $R=0.5$  ml/min on a Si substrate with native (plus plasma-formed)  $\text{SiO}_2$  cladding layer. A number of layers with distinct boundaries are visible, i.e. amorphous  $\text{SiO}_2$ , an amorphous LNT/ $\text{SiO}_2$  intermediate layer (20–25 nm thick) and the crystalline LNT film itself. A similar amorphous intermediate layer of 5–10 nm in

thickness has been reported by Lee and Feigelson [4] for their MOCVD-fabricated LN films on  $\text{SiO}_2/\text{Si}$  substrates. Previously reported LNT films produced by TPS CVD on  $\text{SiO}_2/\text{Si}$  at  $R=4$  ml/min had a 30–35-nm-thick intermediate layer, which implies that its thickness is influenced by the source feeding rate. Therefore, taking into account the results in Fig. 2b, we suppose that the amorphous interlayer thickness and structure can also play an important role in LNT film roughening, and consequently, better control of this layer thickness and structure will positively affect the LNT film quality and properties.

The EDS method employed to determine the chemical composition of well-oriented ( $f=0.90$ )  $\text{LiNb}_{0.2}\text{Ta}_{0.8}\text{O}_3$  film grown at  $R=2$  ml/min and  $T_{\text{sub}}=550$ –560 °C revealed diffusion profiles for Nb and Ta atoms across the interface of the LNT/ $\text{SiO}_2/\text{Si}$  structure, which were similar to those previously reported for  $\text{LiNb}_{0.5}\text{Ta}_{0.5}\text{O}_3$  films [16], with zero Nb and Ta contents within  $\text{SiO}_2$  layer and uniform distribution within the LNT film layer. Taking into account that the accuracy of this analytical method is about  $\pm 5$  at.%, it can be concluded that  $\text{LiNb}_{1-x}\text{Ta}_x\text{O}_3$  film with Ta content  $x=\text{Ta}/(\text{Nb}+\text{Ta})$  of close to 0.8 (or Nb:Ta = 1:4) was fabricated. This is in good agreement with our previous results for sapphire and Si substrates [16,18–20], which revealed good compositional control of TPS-CVD-formed LNT films.

It was found by SEM and TEM analyses that the majority of LNT films exhibited the columnar growth mode. The crystallites observed confirmed the good (0 0 6) orientation, although the in-plane alignment was random for different grains. Also, no secondary phase was detected by high-resolution (HR) TEM near the interface, although some amount of the amorphous phase was found between LNT grains, implying that growth and annealing conditions can be further optimized. HR TEM examination of the film in Fig. 3 confirmed its high degree of texturing. The average grain size was found to be somewhat larger compared with that for the films deposited at  $R=4$  ml/min, which is consistent with the results obtained by Lee and Feigelson [4,5], who also reported that LN grain size decreases at higher growth rates.

As mentioned previously [16], the hexagonal  $c$  lattice constant of the TPS-CVD-prepared  $\text{LiNb}_{1-x}\text{Ta}_x\text{O}_3$  films with  $x=0.5$ , calculated from their XRD patterns on the basis of  $d_{(0\ 0\ 6)}$ , was 13.81–13.83 Å. The newer result for the films with  $x=0.8$  gives 13.78–13.80 Å. Both values are very close to those for the bulk materials (Fig. 4). Our results for the LNT  $c$ -parameters are slightly different from those for sol–gel-derived LNT films on Si(1 1 1) reported by Cheng et al. [9] which are also presented in Fig. 4. They also differ from the result obtained by Bornand et al. [12], whose pyrosol-formed LT films on Si(1 1 1) demonstrated weak com-

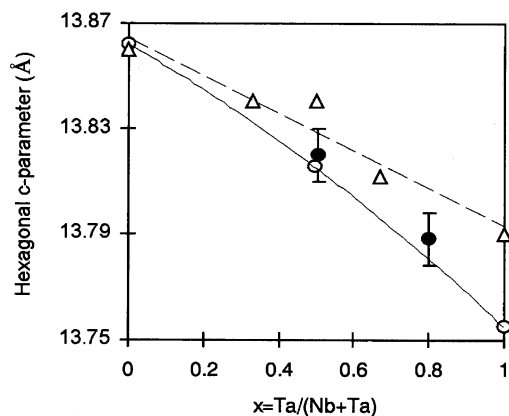


Fig. 4. Variation of the hexagonal cell  $c$  parameter of the deposited LNT films with the  $x = \text{Ta}/(\text{Nb} + \text{Ta})$  ratio of liquid source material used (closed circles). For comparison, three points for bulk materials with  $x = 0, 0.5$  and  $1$  (open circles), as well as five points for sol-gel-derived LNT films on Si(1 1 1) [9] (open triangles) are also presented, the solid line for bulk material and dashed line for sol-gel-derived LNT films are only guides for the eye.

pression along the  $\langle 001 \rangle$  direction ( $c = 13.72 \text{ \AA}$ , whereas for bulk LT material  $c = 13.755 \text{ \AA}$ ). Note that TPS-CVD-fabricated epitaxial LNT films on (0 0 1) sapphire had smaller  $c$ -parameters, which is probably due to the effect of planar tensile stress resulting from the difference in the thermal expansion coefficients of the film and substrate [18–20]. It should also be noted that, in contrast to sol-gel-grown LNT/Si films [9], our LNT films do not demonstrate any dependence of their orientation on the Ta content ( $x = \text{Ta}/(\text{Nb} + \text{Ta})$ ).

Although a single-crystalline film would be of more interest, it is sufficient, for many nonlinear optical applications, that the LNT film be highly (0 0 6)-oriented, since the  $\langle 001 \rangle$  direction is the optical axis of the crystal, and the film with (0 0 6) texture gives a single coefficient elements, such as piezoelectric ( $d_{33}$ ), electro-optic ( $\gamma_{33}$ ), permittivity ( $\epsilon_{33}$ ) and refractive index ( $n_{33}$ ), for the entire film. Therefore, the highly (0 0 6)-oriented but polycrystalline LNT films described here are believed to satisfy the criteria for crystalline quality required for some nonlinear optical and electrooptical applications.

#### 4. Summary

Lithium niobate–tantalate films with the compositions  $\text{LiNb}_{0.5}\text{Ta}_{0.5}\text{O}_3$  and  $\text{LiNb}_{0.2}\text{Ta}_{0.8}\text{O}_3$  and with very high (0 0 6) orientation have been grown on Si(1 0 0) substrates by the thermal plasma spray CVD method. It was demonstrated that the source material liquid feeding rate, along with deposition temperature, is the key factor governing film orientation and surface roughness. The high (0 0 6) orientation seems to result from the growth-

rate anisotropy effect. Further experimental investigations on nucleation and growth mechanisms are required in order to improve the surface smoothness and film crystallinity. In contrast to sol-gel-grown LNT/Si films, TPS-CVD-fabricated films on Si do not demonstrate any dependence of their orientation on the Nb/Ta ratio. Their (0 0 6) orientation is influenced mainly by the deposition temperature and growth rate. The LNT films described may be useful in integrated optical devices, pyroelectric devices, and metal-ferroelectric-semiconductor nonvolatile memory applications.

#### Acknowledgments

S.A.K. acknowledges the support of the Japan Society for the Promotion of Science (JSPS). This work was financially supported by JSPS under the program 'Research for the Future' (JSPS-RFTF Grant No. 97R15301).

#### References

- [1] J. Ravez, C. R. Acad. Sci., Ser. IIC: Chim. 3 (2000) 267.
- [2] D.K. Fork, F. Armani-Leplingard, J.J. Kingston, MRS Bull. 21 (7) (1996) 53.
- [3] M.K. Francombe, S.V. Krishnaswamy, J. Vac. Sci. Technol. A. 8 (1990) 1382.
- [4] S.Y. Lee, R.S. Feigelson, J. Mater. Res. 14 (1999) 2662.
- [5] S.Y. Lee, R.S. Feigelson, J. Cryst. Growth 186 (1998) 594.
- [6] R.E. Cohen, J. Phys. Chem. Solids 61 (2000) 139.
- [7] D. Xue, K. Betzler, H. Hess, Solid State Commun. 115 (2000) 581.
- [8] X.L. Guo, Z.G. Liu, S.N. Zhu, T. Yu, S.B. Xiong, W.S. Hu, J. Cryst. Growth 165 (1996) 187.
- [9] S.D. Cheng, C.H. Kam, Y. Zhou, X.Q. Han, W.X. Que, Y.L. Lam, Y.C. Chan, J.T. Oh, W.S. Gan, Thin Solid Films 365 (2000) 77.
- [10] C.H.J. Huang, T.A. Rabson, Optics Lett. 18 (1993) 811.
- [11] D. Ghica, C. Ghica, M. Gartner, V. Nelea, C. Martin, A. Cavaleru, I.N. Mihailescu, Appl. Surf. Sci. 138/139 (1999) 617.
- [12] V. Bornand, Ph. Papet, E. Philippot, Thin Solid Films 304 (1997) 239.
- [13] S.D. Cheng, Y. Zhou, C.H. Kam, X.Q. Han, W.X. Que, Y.L. Lam, Y.C. Chan, J.T. Oh, W.S. Gan, Mater. Lett. 44 (2000) 125.
- [14] Z.C. Wu, W.S. Hu, J.M. Liu, M. Wang, Z.G. Liu, Mater. Lett. 34 (1998) 332.
- [15] W.S. Hu, Z.G. Liu, Z.C. Wu, J.M. Liu, X.Y. Chen, D. Feng, Appl. Surf. Sci. 141 (1999) 197.
- [16] S.A. Kulinich, J. Shibata, H. Yamamoto, Y. Shimada, K. Terashima, T. Yoshida, Appl. Surf. Sci. 182 (2001) 150.
- [17] N. Yamaguchi, T. Hattori, K. Terashima, T. Yoshida, Thin Solid Films 316 (1998) 185.
- [18] T. Majima, H. Yamamoto, S.A. Kulinich, K. Terashima, J. Cryst. Growth 220 (2000) 336.
- [19] H. Yamamoto, S.A. Kulinich, K. Terashima, Thin Solid Films 390 (2001) 1.

- [20] D.V. Shtansky, S.A. Kulinich, K. Terashima, T. Yoshida, Y. Ikuhara, *J. Mater. Res.* 16 (2001) 2271.
- [21] T.A. Rost, H. Lin, T.A. Rabson, R.C. Bauman, S.L. Callahan, *J. Appl. Phys.* 72 (1992) 4336.
- [22] V. Bouquet, E. Longo, E.R. Leite, J.A. Varela, *J. Mater. Res.* 14 (1999) 3115.
- [23] S. Ono, S. Hirano, *J. Mater. Res.* 16 (2001) 1155.
- [24] G. Carter, *Vacuum* 56 (2000) 87.
- [25] G. Knuyt, C. Quaeys, J. D'Haen, L.M. Stals, *Thin Solid Films* 258 (1995) 159.